[Ag-20S2P(OR)(2)(12)]: A Superatom Complex with a Chiral Metallic Core and High Potential for Isomerism

Rajendra S. Dhayal, Yan-Ru Lin, Jian-Hong Liao, Yuan-Jang Chen, Yu-Chiao Liu, Ming-Hsi Chiang, Samia Kahlal, Jean-Yves Saillard, C. W. Liu

$[Ag_{20}\{S_2P(OR)_2\}_{12}]$: A Superatom With Chiral Metallic Core and Rich Isomerism Potentialities**

Rajendra S. Dhayal, Yan-Ru Lin, Jian-Hong Liao, Yuan-Jang Chen, Yu-Chiao Liu, Ming-Hsi Chiang, Samia Kahlal, Jean-Yves Saillard* and C. W. Liu*

[∗] Dr. R. S. Dhayal, Y.-R. Lin, J.-H. Liao, Prof. C. W. Liu
Department of Chemistry, National Dong Hwa University
No. 1, Sec. 2, Da Hsueh Rd., Shoufeng, Hualien 97401, Taiwan, R.O.C.
Fax: (+886)3-863-3570
E-mail: chenwei@mail.ndhu.edu.tw
Homepage: http://faculty.ndhu.edu.tw/~cwl/index.htm
Dr. R. S. Dhayal
 Centre for Chemical Sciences, School of Basic and Applied Sciences, Central University of Punjab, Bathinda-151 001, India
Dr. S. Kahlal, Prof. J.-Y. Saillard
UMR-CNRS, 6226 "Institut des Sciences Chimiques de Rennes", Université de Rennes 1, 35042 Rennes Cedex, France.
Dr. Y.-C. Liu, Dr. M.-H. Chiang
Institute of Chemistry, Academica Sinica, Taipei, Taiwan, R.O.C.
Prof. Y.-J. Chen
 Department of Chemistry, Fu Jen Catholic University, New Taipei City 24205, Taiwan, R. O. C.

Abstract

Herein we present the synthesis and the first structural determination of a silver nanocluster $[Ag_{20}\{S_2P(O^iPr)_2\}_{12}]$, **2**, which contains an intrinsic chiral metallic core and is produced via reduction of one silver ion from the eight-electron superatom $[Ag_{21}\{S_2P(O^iPr)_2\}_{12}](PF_6)$, **1**, by borohydrides. Single crystal X-ray analysis displays an Ag_{20} core of pseudo C_3 symmetry comprising a silver-centered Ag_{13} icosahedron capped by seven silver atoms. Its n-propyl derivative, $[Ag_{20}\{S_2P(O^nPr)_2\}_{12}]$ (**3**), can also be prepared by the treatment of silver(I) salts and dithiophosphates in a stoichiometric ratio in the presence of excess amount of $[BH_4]^-$. Astonishingly crystal structure analyses reveal that the capping silver-atom positions relative to their icosahedral core are distinctly different in **2** and **3** and generate isomeric, chiral Ag_{20} cores. Both Ag_{20} clusters display an emission maximum in the near IR region. DFT calculations are consistent with a description within the superatom model of an 8-electron $[Ag_{13}]^{5+}$ core protected by a $[Ag_7\{S_2P(OR)_2\}_{12}]^{5-}$ external shell. Moreover, two additional structural variations are predicted by DFT, showing isomerism potentialities for such $[Ag_{20}\{S_2P(OR)_2\}_{12}]$ species.

Atomically precise noble metal nanoclusters of which structures were determined by single crystal X-ray diffraction have been very challenging to pursue, due to difficulties in the growth of single crystals of appropriate quality. However, owing to their potential applications in multidisciplinary fields such as catalysis, luminescence, sensing, electronics, and biology,[1-3] they remain highly topical. In the past few years, significant progresses have been made in the single-crystal structure study of gold nanoclusters[3] protected by Au-thiolate staple units, such as Au_{102},[4] Au_{133},[5] Au_{38},[6] Au_{36},[7] Au_{30},[8] Au_{28},[9] and Au_{25}.[10] Among these clusters, the Au_{102}, Au_{38}, and Au_{28} cores are chiral due to asymmetric arrangement of the Au-thiolate staple units. A chiral Au_{20} core of C_3 symmetry was also revealed in $[Au_{20}(PP_3)_4]Cl_4$ (P = tetradentate phosphine), which consists of a centered-icosahedral Au_{13} capped by seven Au atoms in a helical Y-shape.[11] Besides the aforementioned investigations, the structural isomerism study at nanoscale in $Au_{28}(SR)_{20}$ (R = -c-C_6H_{11}, -Ph-^tBu)[12] has opened up an exciting new avenue for nanostructure researches. Even though isomers lying close in energy have been predicted in Ag clusters based on DFT study,[13] structurally characterized isomeric silver nanoclusters remain unknown.

The structural diversity identified in gold nanoclusters inspires scientists to develop silver analogues. The unusual stability of the $M_4Ag_{44}(SPh)_{30}$ (M = alkali metal) nanoclusters[14] was attributed to an 18-electron superatomic closed-shell configuration. More recently, Bakr *et. al.* reported the structures of $[Ag_{25}(SR)_{18}]^-$ and $[Ag_{29}(BDT)_{12}(TPP)_4]$, where an Ag_{25} structure was found virtually identical to that of $[Au_{25}(SR)_{18}]^-$.[15] Subsequently there were reports on doped thiolate silver nanoparticles, $[MAg_{24}(SR)_{18}]^{2-}$ (M = Pt, Pd)[16] and $[AuAg_{24}(SR)_{18}]^-$,[17] characterized by X-ray diffraction. Interestingly, intercluster reactions between $Au_{25}(SR)_{18}$ and $[Ag_{44}(SR)_{30}]^{4-}$ reveals the formation of $[Au_{25-x}Ag_x(SR)_{18}]$ (x = 0-20), which are primarily characterized by mass spectrometry.[18] However to the best of our knowledge *there has been no reported structural evidence on a superatom-type silver nanocluster having a chiral inorganic core.* Indeed, nanoscale chirality is of immense interest due to varieties of applications such as enantioselective catalysis, chiro- optical devices, *etc.*[19, 20]

Our group has a strong interest in pursuit of group 11 nanoparticle formation pathways made via wet chemical reduction methods. Along this direction, we have successfully characterized several copper hydrides stabilized by bidentate dichalcogen (S/Se) ligands (L)[21] as well as hydrido silver (or copper) clusters en route to the ultimate metal nanoparticles from which assumptions on the existence of various alloy clusters as key intermediates were proposed.[22] Eventually, the first eight-electron silver nanocluster $[Ag_{21}\{S_2P(O^iPr)_2\}_{12}](PF_6)$, **1**,[23] was isolated in the series. Bearing in mind that a chiral superatom may be produced through removal of one peripheral silver ion from the Ag_{21} core of **1**, we report herein the new $[Ag_{20}\{S_2P(O^iPr)_2\}_{12}]$ cluster, **2**, that is merely one silver atom smaller than the previous Ag_{21} cluster. The new Ag_{20} cluster core, which exhibits interesting differences in structural features and optical properties from those of the Ag_{21} cluster, consists of an intrinsic chiral inorganic core, a combination of a centered-icosahedral Ag_{13} nucleus and seven capping silver atoms, to retain eight electrons in agreement with the unified superatom concept.[24]

The initial synthesis of pure $[Ag_{20}\{S_2P(O^iPr)_2\}_{12}]$, **2**, which is air- and moisture-stable, started with $[Ag_{21}\{S_2P(O^iPr)_2\}_{12}](PF_6)$, **1** by dissolving it in tetrahydrofuran (THF) (see supporting information). The resulting solution was cooled to -20 °C for 20 minutes and $NaBH_4$ solution (a mixture of DMF and THF in a 1:4 ratio) was then added quickly. After 1h, solvents were removed under reduced pressure and the obtained brown-red solid was extracted in sufficient amount of hexane. The fractions of hexane were combined and dried to yield pure **2**. Alternatively, a direct synthesis of **2** was developed by treating Ag^+ salts and dithiophosphates (dtp) in stoichiometric ratios in the presence of excess amount of $[BH_4]^-$ (see supporting information). A *n*-propyl derivative, $[Ag_{20}\{S_2P(O^nPr)_2\}_{12}]$, **3**, can be generated by the latter method. Both **2** and **3** are quite stable in non-polar solvents but decompose in a few hours specifically in chlorinated solvents, whereas nanocluster **2** regenerated into **1**. Both **2** and **3** were structurally characterized by single-crystal X-ray diffraction and their compositions were confirmed by electrospray ionization mass spectrometry (ESI-MS), multinuclear NMR, X-ray photoelectron spectroscopy (XPS), UV/Vis, and EDS for the Ag:S atomic ratio. Furthermore, DFT and TDDFT investigations provide a rationalization of their structure, bonding, stability and optical properties.

The positive ESI-MS spectrum of **2** shows a molecular ion peak at *m/z* 4716.3 (calcd 4716.3), corresponding to the molecular weight of neutral $[Ag_{20}\{S_2P(O^iPr)_2\}_{12}]$ (Fig 1a). By analyzing its isotopic pattern, the ionized nanocluster was determined to be mono-charged because the isotope peak spacing is unity (+1) (inset of Fig 1a). Additional peaks in lower and higher mass ranges can be attributed to a fragment $[Ag_{20}\{S_2P(O^iPr)_2\}_{11}]^+$ (*m/z* 4503.3) and the adduct $[Ag_{21}\{S_2P(O^iPr)_2\}_{12}]^+$ (*m/z* 4823.2), respectively. The UV-vis spectrum of **2** shows broad multiband optical absorption bands (at 260, 360, 435, 443, and 492 nm) and one shoulder band at 540 nm (Fig 1b, S1 and Table S1), whereas the same number of absorption band with shifted positions (at 235, 260, 381, 425, 482 and 540 nm) were also observed in **1**. Both **1** and **2** exhibit luminescence in the near-IR region ~921 nm and ~ 950 nm, respectively. The XPS of **2** shows the existence of both Ag^0 and Ag^I. The Ag $3d_{5/2}$ XPS peak can be resolved into two peaks at binding energies of 367.63 eV and 368.73 eV (Fig S2), corresponding to Ag^I and Ag^0, respectively.[25] Further, EDS results of **2** showed Ag and S atomic ratio to be 46.67:53.33 (calc.46.66:53.33) (Fig S3, Table S2).

The crystallization of **2** was performed by vapor diffusion of hexane into a concentrated acetone solution at 4 °C. Rectangular-shaped dark-red crystals of **2**, which crystallize in monoclinic $P2_1/n$ space group, were obtained in a couple weeks. Fig 2a represents an entire structure of $[Ag_{20}\{S_2P(O^iPr)_2\}_{12}]$. The unit cell consists of

enantiomeric pairs similar to the reported chiral gold nanoclusters (Au_{102}, Au_{38} and Au_{28})[3] and this is the reason why no optical activity is revealed in its CD spectrum.[8] It has an idealized C_3 symmetry with the 3-fold axis passing through atoms Ag20, Ag1 and the center of two Ag_3 triangles (Fig 2a). The architecture of **2** exhibits an Ag_{20} kernel stabilized by twelve dtp ligands. The metal core comprises an Ag-centered Ag_{13} icosahedron capped by seven Ag atoms. The icosahedron can be seen as a ring of six silver atoms in a chair form, sandwiched between two staggered Ag_3 triangular faces along the pseudo C_3 axis (side view in Fig 2b). The capping Ag atoms occupy seven of the twenty triangular faces of the icosahedron, in such a way that one of them (Ag14) lies on the C_3 axis and the remaining six locate around the C_3 axis to form three butterfly groups, where hinges are made by alternative side edges of the Ag_6 chair (Fig 2c). Alternatively, a view along the pseudo C_3 axis of Figure 2d reveals that three groups of capping Ag atoms represent two almost coplanar triangles in a closed to eclipsed position (staggering angle: 18.7°) in a 3-fold propeller-like shape. The radial and peripheral Ag-Ag distances within the silver-centered Ag_{13} icosahedron are in the range 2.7299(5) - 2.8244(5) Å and 2.8605(5) - 3.0111(5) Å, respectively. These distances are shorter than the Ag-Ag distances (2.9171(5) – 3.0266(5) Å) between Ag_{ico} and capping (μ_3-Ag) atoms. The ranges in every type of Ag-Ag distances increase in comparison with the corresponding distances in **1** (2.7542(8)-2.8159(8) Å, 2.8420(9)-2.9980(9) Å and 2.813(5)-2.846(5) Å, respectively), indicating a slight expansion of the Ag_{20} metallic core.
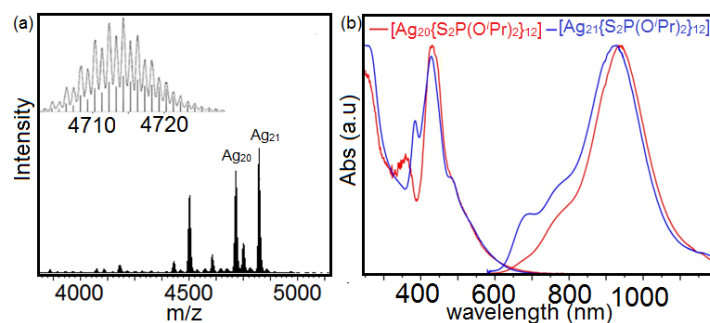

Figure 1. (a) ESI-MS spectrum of **2**. The inset shows the experimental (top) and theoretical one (bottom). (b) UV-vis absorption (left-side) and normalized emission (right-side) spectra of **1** and **2** in chloroform.
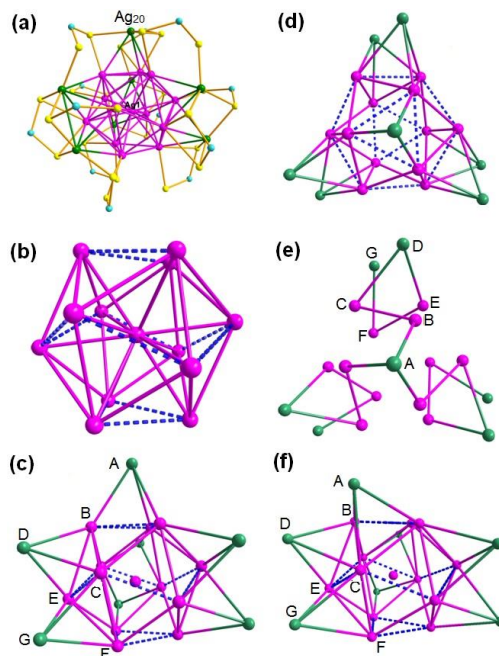

Figure 2. (a) Full molecular structure of **2** (isopropoxy groups omitted for clarity). (b) The Ag-centered Ag_{13} icosahedron (pink spheres) made of an Ag_6 ring in a chair form sandwiched between two Ag_3 triangles in relative staggered conformation (dashed edges in blue). (c) Out of seven capping Ag atoms (green spheres), six are making butterflies around the C_3 axis with hinge positions being alternative edges of the Ag_6 chair, and labelling of different surface atom types (A-G). (d) A top view of the Ag_{20} core, where six capping atoms participate in three-fold propeller. (e) A top views of the three clockwise silver strands constituting the Ag_{20} core. (f) The Ag_{20} core of **3**, where the capping atom (A), whichlies at the C_3 axis in **2** (fig **2**c) is now completely off theaxis. Ag (pink and green), S (yellow), P (cyan).

The relationship between the molecular structures of **1** and **2** is straightforward. Whereas **1** exhibits an Ag_{21} core of idealized D_3 symmetry, one of the two capping silver atoms situated on the three-fold axis is missing in **2**, lowering the symmetry to C_3, but leaving the remaining cluster topology as a whole basically unchanged. Additionally, there are interactions (3.285 – 3.382 Å) between the capping silver atoms and the wing tips of neighboring butterfly group, which are also observed in **1** and smaller than the sum of Van der Waals radii for silver (3.40 Å).[26] A centered icosahedron was also structurally identified in silver nanoclusters stabilized by either thiolated or mixed thiol-phosphine ligand systems such as Ag_{25} and Ag_{29},[15] whereas an empty Ag_{12} icosahedron is present in Ag_{44} thiolato-stabilized species.[14]
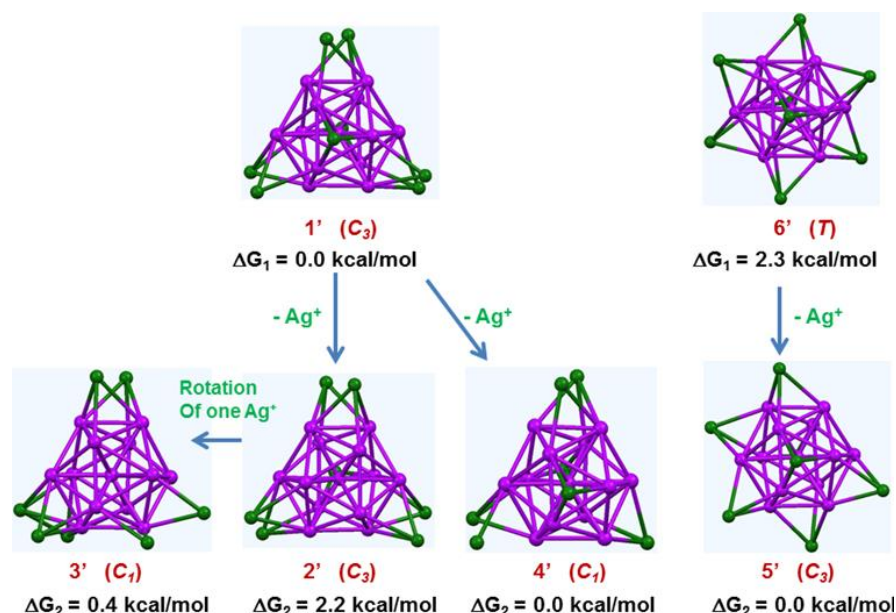

Figure 3. Structural relationships of the metallic cores in the $[Ag_{21}\{S_2PH_2\}_{12}]^+$ (**1'**, **6'**) and $[Ag_{20}\{S_2PH_2\}_{12}]$ (**2'-5'**) isomers. ΔG_1 and ΔG_2 are the relative free energies at 298 K of the Ag_{21} and Ag_{20} species, respectively. Ideal symmetries refer to the entire clusters (including the ligands).

The The Ag_{20} core of **2** represents an unprecedented chiral arrangement of silver atoms as shown in Fig 2c, where the 19 surface Ag atoms can be classified into seven types of symmetry-related atoms (A-G) in a ratio of 1:3:3:3:3:3:3. Three groups of every single Ag atom type create three clockwise helices along the C_3 axis (Fig 2e). *To the best of our knowledge this is the first structural evidence for a silver nanocluster bearing an intrinsic chiral metallic core.* Its structural features are somehow similar to a recently discovered tetradentate phosphine-stabilized gold nanocluster, where an Au_{20} core of C_3 symmetry also has an intrinsic chiral inorganic core.[11] However in this Au_{20} core, the seven capping Au atoms constitute a helical Y-shape over the centered icosahedron Au_{13} and its electron count is also different from that of **2**.

The Ag_{20} framework in **2** is stabilized by twelve dtp ligands through three spherical rows (top, middle and bottom) in a ratio of 3:6:3 around the pseudo C_3 axis (Fig 2a). The ligands in top and middle spherical rows show trimetallic (η^3) connectivity with one Ag_{ico} and two Ag_{cap} atoms via tri (μ_2, μ_1) and tetra (μ_2, μ_2) coordination modes, whereas ligands at the bottom row have dimetallic tri-connectivity (η^2: μ_2, μ_1) with one Ag_{ico} and one Ag_{cap} atoms due to the loss of one capping atom, as compared to **1**. The ligands in middle spherical row have alternatively both trimetallic tetraconnectivity (η^3: μ_2, μ_2) and trimetallic triconnectivity (η^3: μ_2, μ_1) patterns. The bond distances Ag_{cap}-S (avg. 2.51 Å) and the S…S bite (avg. 3.401(5)) Å in **2** are identical to their corresponding distances in **1**, but the Ag_{ico}-S bond distances are longer (avg. 2.72 Å) in comparison with those of Ag_{21} (avg. 2.670 Å).

Among the 19 surface atoms of the Ag_{20} core (labeled A-G in Fig 2c), the A-, D- and G-type (Ag_{cap}) atoms are bonded to three S atoms in a near trigonal planar conformation, the B-, E- and F-type (Ag_{ico}) atoms to two and the C-type (Ag_{ico}) atoms to only one. Accordingly, four types of phosphorous ligands are authenticated by the ^{31}P NMR spectrum of **2** with the appearance of four resonances at 105.21, 104.09, 102.74, 100.33 ppm in an equal integration ratio at -70 °C, whereas only one broad resonance centered at 101.87 pm was observed at 22 °C (Fig S4a, b). Thus, ^{31}P NMR study supports the existence of chirality in the nanocluster in solution.

The anatomy of the Ag_{20} cores in **3** exhibits a singular difference, as compared to that of **2**. It concerns the location of the capping silver atoms denoted A (Fig 2c, f). Whereas in **2**, AgA lies on the C_3 axis, it is completely off this axis in **3**, in such a way that the idealized C_3 symmetry is now broken (Fig 2f). This effect is likely due to the peculiar steric hindrance of the ^{n}Pr alkyl groups. *These results indeed provide an important lesson: that is*

4

atomically precise nanoclusters may have different structures even though their compositions are almost identical.

DFT calculations[27] have been carried out at the BP86/Def2-TZVP level on simplified models of formula $[Ag_{20}\{S_2PH_2\}_{12}]$. Starting the geometry optimization from the crystal structure of **2** or from the structure of the C_3 $[Ag_{21}\{S_2PH_2\}_{12}]^+$ model[22] (**1'**) to which one of the Ag^+ ions lying on the C_3 axis has been removed, yielded the same energy minimum of nearly C_3 symmetry (**2'**), analogous to the experimental structure of **2** (see Supporting Information). Consistently with its superatom nature, a substantial HOMO-LUMO gap of 1.52 eV is computed for **2'**, which compares well with that of **1'** (1.68 eV). Whereas the optimized Ag-Ag distances in **2'** are, unsurprisingly,[22c, 23] somewhat longer than their corresponding experimental counterparts, they follow the same trend. Within the icosahedron they range 2.850 Å –2.947 Å (Ag_{center}-Ag_{ico}) and 2.942 Å – 3.201 Å (Ag_{ico}-Ag_{ico}). The Ag_{cap}-Ag_{ico} distances are as follow: Ag(A)–Ag_{ico} = 3.081 Å, Ag(D)-Ag_{ico}= 3.096 Å (avg.), Ag(D)-Ag(E)= 2.956 Å. In the latter case, the capping atom is found to be in reasonably close contact with only one Ag_{ico} atom (of type E), contrarily to what shows the X-ray structure of **2**. The expansion of the Ag_{20} core when going from the experimental to the optimized structure causes the Ag(E) atoms to be bonded to only one sulfur atom in **2'**, whereas in **2** they are bonded to two (see above), one of the experimental Ag(E)-S distances being however quite long (2.9369(13) Å). The Wiberg bond indices computed in **2'** follow the structural trends, *i.e.* 0.337 (avg.) and 0.083 (avg.) for the Ag_{center}-Ag_{ico} and Ag_{ico}-Ag_{ico} bonds, respectively. The Ag_{ico}-Ag_{ico} values, averaging 0.032, are significantly lower. As in the case of **1**,[23] this is consistent with the view of an icosahedral $[Ag_{13}]^{5+}$ superatom system associated with the eight metal electrons in a spherical jellium $1S^2 1P^6$ configuration,[24] surrounded by an $[Ag_7(dtp)_{12}]^{5-}$ protecting shell in which the seven Ag_{cap} atoms are in the +I oxidation state, and interact with the icosahedron mainly through metallophilic weak interactions. This view is also supported by the metal computed natural atomic charges (-0.47, +0.24 (avg.) and +0.62 (avg.) for Ag_{center}, Ag_{ico} and Ag_{cap} respectively. Moreover, it was possible to identify molecular orbitals of **2'** which can be associated with the frontier jellium levels (see Fig S5).

Geometry optimization of the $[Ag_{20}\{S_2PH_2\}_{12}]$ model starting from the X-ray structure of **3** led to an energy minimum **3'** (HOMO-LUMO gap of 0.52 eV) of similar topology which lies only 1.8 kcal/mol below **2'** (free energy). Its core electronic structure is similar to that of **3'**.

As mentioned above, the structure of **2** (or **2'**) can be derived from that of **1** (or **1'**) by simply removing one of its capping Ag^+ atoms. However, there are two types of capping atoms in **1** (or **1'**): the two lying on the C_3 axis and the six other ones. Removing one of the latter atoms generates a structure of C_1 symmetry, of different topology from that of **2** (or **2'**) (Fig 3). Optimization of this structure for the $[Ag_{20}\{S_2PH_2\}_{12}]$ model yielded an isomer **4'** being 2.2 kcal/mol below **2'**. Moreover, another energy minimum, differing from **2'**, **3'** and **4'** by the way the seven capping atoms are distributed around the Ag_{13} icosahedron was found. This isomer of C_3 symmetry (**5'**) is computed to be isoenergetic with **4'**. Thus, the four computed isomers lie within a range of 2.2 kcal/mol in free energy, a value hardly significant at our level of modelization. Interestingly, the structure of **5'** can be derived from that of a hypothetical isomer of **1'** of T symmetry (labeled **6'**), by removing one of its eight symmetry-equivalent capping Ag^+ atoms. **6'** is computed to be 2.3 kcal/mol above **1'**. The structural relationships of the **1'**-**6'** species are summarized in Fig 3. They all possess the same $[Ag_{13}]^{5+}$ superatomic core and similar arrangement of their ligand coverage. They mainly differ by the location of their seven (or eight) Ag^+ capping atoms. These results suggest that several structural types of $[Ag_{20}\{S_2P(OR_2)\}_{12}]$ compounds are possible, all with the same superatomic icosahedral $[Ag_{13}]^{5+}$ nucleus, but different distribution of their 7 Ag^I atoms. In the case of isomers, they should exhibit somewhat different optical properties, as exemplified by the TDDFT-simulated UV-vis spectra of **2'-5'** shown in Fig S6. The major optical transitions of lowest energy determined for **2'** by TDDFT calculations are found at 459, 484, 532 and 598 nm. They can be assigned to MLCT, LMCT, MMCT and MMCT, respectively. The transition at 598 nm has a rather low oscillating factor and thus is expected of weak intensity. The three other values fit reasonably well with the bands observed for **2** at 435, 443 and 492 nm. The TDDFT-computed CD spectra of the **2'** enantiomers are shown in Fig. S7. The high energy feature at ~ 420 nm is of strong MLCT nature, whereas the low energy one at ~ 625 nm is due to MMCT transitions presenting significant (~ 10-20%) Ag_{center}/Ag_{ico} → Ag_{cap} character.

In summary, new nanoclusters $[Ag_{20}\{S_2P(OR)_2\}_{12}]$ (R = ^iPr, ^nPr) with isomeric, chiral metallic core have been obtained and structurally characterized. The structure of **2** (R = ^iPr) can be derived from that of **1** by simply removing one of the capping atoms lying on the C_3 axis, with only minor additional changes in the overall connectivity and shape of the molecule. This is reminiscent of the structural and chemical relationships between $[M_8(H)\{E_2P(OR)_2\}_6]^+$ and $[M_7(H)\{E_2P(OR)_2\}_6]$ (M = Cu, Ag; E = S, Se).[21d] The structure of cluster **3** (R = ^nPr) can be derived from that of **2** by simply shifting off the capping atom lying on the C_3 axis, generating a chiral structure of C_1 symmetry and revealing structural isomerism in the Ag_{20} core. The denticity (tetra *vs* bidentate) of phosphine and dithiolate ligands used to protect the metallic core plays a key role on the adopted structural distinctions between the intrinsic Ag_{20} and Au_{20}[11] chiral cores. The phenomenon of denticity provides a strong impetus for further work using bidentate ligands to modulate the structures of silver and gold nanoclusters. DFT calculations indicate that the stability of the Ag_{20} nanoclusters can be rationalized as that of an 8-electron superatom, composed of an $[Ag_{13}]^{5+}$ nucleus stabilized by an $[Ag^I_7\{S_2P(OR)_2\}_{12}]^{5-}$ covering shell. Calculations suggest that the shape flexibility of this outer shell can potentially enable to generate low-energy isomers for which different properties might be expected.

REFERENCES

[1] a) M.-C. Daniel, D. Astruc, *Chem. Rev*. **2004**, *104*, 293–346; b) R. R. Arvizo, S. Bhattacharyya, R. A. Kudgus, K. Giri, R. Bhattacharya, P. Mukherjee, *Chem. Soc. Rev.* **2012***, 41*, 2943–2970.

[2] a) J. Sharma, R. Chhabra, A. Cheng, J. Brownell, Y. Liu, H. Yan, *Science,* **2009***, 323*, 112–116; b) C. M. Niemeyer, *Angew. Chem.***2001**, *113*, 4254–4287; *Angew. Chem. Int. Ed*. **2001**, *40*, 4128–4158; c) M. A. Noginov, G. Zhu, A. M. Belgrave, R. Bakker, V. M. Shalaev, E. E. Narimanov, S. Stout, E. Herz, T. Suteewong, U. Wiesner. *Nature* **2009**, *460*, 1110–1112; d) H. A. Atwater, A. Polman, *Nature Mater.* **2010**, *9*, 205–213.

[3] R. Jin, Nanoscale, **2015**, *7*, 1549-1565.

[4] P. D. Jadzinsky, G. Calero, C. J. Ackerson, D. A. Bushnell, R. D. Kornberg, Science **2007**, *318*, 430 – 433.

[5] a) C. Zeng, Y. Chen, K. Kirschbaum, K. Appavoo, M. Y. Sfeir, R. Jin, *Sci. Adv.* **2015**, *1*, e1500045; b) A. Dass, S. Theivendran, P. R. Nimmala, C. Kumara, V. R. Jupally, A. Fortunelli, L. Sementa, G. Barcaro, X. Zuo, B. C. Noll, *J. Am.Chem. Soc.* **2015**, *137*, 4610–4613.

[6] H. Qian, W. T. Eckenhoff, Y. Zhu, T. Pintauer, R. Jin, *J. Am. Chem. Soc*. **2010**, *132*, 8280–8281.

[7] C. Zeng, H. Qian, T. Li, G. Li, N. L. Rosi, B. Yoon, R. N. Barnett, R. L. Whetten, U. Landman, R. Jin, *Angew. Chem.* **2012**, *124*, 13291 – 13295; *Angew. Chem. Int. Ed*. **2012**, *51*, 13114 – 13118.

[8] D. Crasto, S. Malola, G. Brosofsky, A. Dass, H. Häkkinen, *J. Am. Chem. Soc*. **2014**, *136*, 5000-5005.

[9] C. Zeng, T. Li, A. Das, N. L. Rosi, R. Jin, *J. Am. Chem. Soc*. **2013**, *135*, 10011 – 10013.

[10] a) M. W. Heaven, A. Dass, P. S. White, K. M. Holt, R. W. Murray, *J. Am. Chem. Soc*. **2008**, *130*, 3754 – 3755; b) M. Zhu, C. M. Aikens, F. J. Hollander, G. C. Schatz, R. Jin, *J. Am. Chem. Soc*. **2008**, *130*, 5883 – 5885; c) J. Akola, M. Walter, R. L. Whetten, H. H_kkinen, H. Gronbeck, *J. Am. Chem. Soc.***2008**, *130*, 3756 – 3757.

[11] X.-K. Wan, S.-F. Yuan, Z.-W. Lin, Q.-M. Wang, *Angew. Chem. Int. Ed.***2014**, *53*, 2923-2926; *Angew. Chem.* **2014**, *126*, 2967- 2970.

[12] Y. Chen, C. Liu, Q. Tang, C. Zeng, T. Higaki, A. Das, D.-E. Jiang, N. L. Rosi, R. Jin, *J. Am. Chem. Soc*. **2016**, *138*, 1482−1485.

[13] a) C. Sieber, J. Buttet, W. Harbich, C. Félix, R. Mitrić, V. Bonačić-Koutecký, *Phys. Rev. A* **2004**, *70*, 41201-41204; b) H. Dhillon, R. Fournier, *Comp. Theor. Chem*. **2013**, *1021*, 26–34; c) R. Fournier, *J. Chem. Phys.*, **2001**, *115*, 2165-2177; d) E. M. Fernández, J. M. Soler, I. L. Garzón, L. C. Balbá *Int. J. Quant. Chem.* **2005**, *101*, 740–745.

[14] a) A. Desireddy, B. C. Conn, J. Guo, B. Yoon, R. N. Barnett, B. M. Monahan, K. Kirschbaum, W. P. Griffith, R. L. Whetten, U. Landman, T. P. Bigioni, *Nature*, **2013**, *501*, 399–402; b) H. Yang, Y. Wang, H. Huang, L. Gell, L. Lehtovaara, S. Malola, H. Hakkinen, and N. Zheng, *Nature Commun*, **2013**, *DOI: 10.1038/ncomms3422*; c) L. G. AbdulHalim, N. Kothalawala, L. Sinatra, A. Dass, O. M. Bakr,*J. Am. Chem. Soc.***2014**, *136*, 15865-15868.

[15] a) C. P Joshi, M. S. Bootharaju, M. J. Alhilaly, O. M. Bakr, *J. Am. Chem. Soc.* **2015**, *137*, 11578−11581; b) L. G. AbdulHalim, M. S. Bootharaju, Q. Tang, S. d. Gobbo, R. G. AbdulHalim, M. Eddaoudi, D.-E. Jiang, O. M. Bakr, *J. Am. Chem. Soc.***2015**, *137*, 11970−11975.

[16] J. Y. Haifeng, H. Su, H. Yang, S. Malola, S. Lin, H. Häkkinen, N. Zheng, *J. Am. Chem. Soc*. **2015**, *137*, 11880−11883.

[17] M. S. Bootharaju, C. P. Joshi, M. R. Parida, O. F. Mohammed, O. M. Bakr, *Angew. Chem. Int. Ed*. **2016**, 55, 922-926; *Angew. Chem.* **2016**, *128*, 934-938.

[18] K. R. Krishnadas, A. Ghosh, A. Baksi, I. Chakraborty, G. Natarajan, T. Pradeep, *J. Am. Chem. Soc*. **2016**, *138*, 140–148.

[19] N. Cathcart, P.Mistry, C. Makra, B. Pietrobon, N. Coombs, M. Jelokhani-Niaraki, V. Kitaev, *Langmuir* **2009,** *25,*5840-5846.

[20] a) V. J. Kitaev, *J. Mater. Chem*. **2008**, *18*, 4745-4749; b) M. Farrag, M. Tschurl, U. Heiz, *Chem. Mater.***2013**, *25*, 862-870.

[21] a) R. S. Dhayal, J.-H. Liao, Y.-R.Lin, P.-K.Liao, S. Kahlal, J.-Y.Saillard, C.W. Liu, *J. Am. Chem. Soc*. **2013**, *135*, 4704-4707; b) J.-H. Liao, R. S. Dhayal, X. Wang, S. Kahlal, J.-Y. Saillard, C. W. Liu, *Inorg. Chem.* **2014**, *53*, 11140-11145; c) A. J. Edwards, R. S. Dhayal, P.-K.Liao, J.-H.Liao, M.-H.Chiang, R. O. Piltz, S. Kahlal, J.-Y.Saillard, C. W. Liu, *Angew. Chem. Int. Ed.* **2014**, *53,* 7214-7218; *Angew. Chem.* **2014**, *126*, 7342-7346; d) R. S. Dhayal, J.−H. Liao, S. Kahlal, X. Wang, Y.-C.Liu, M.-H.Chiang, W. E. van Zyl, J.-Y.Saillard, C. W. Liu, *Chem. Eur. J.* **2015**, *21*, 8369-8374; e) R. S. Dhayal, J.−H. Liao, X. Wang, Y.-C. Liu, M.-H.Chiang, S. Kahlal, J.-Y.Saillard, C. W. Liu, *Angew. Chem. Int. Ed.* **2015**, *54,* 13604-13608; *Angew. Chem.* **2015**, *127*, 13808-13812; f) R. S. Dhayal, W. E. van Zyl, C. W. Liu, *Acc. Chem. Res.* **2016**, 49, 86-95; g) P. V. V. N. Kishore, J.-H. Liao, H.-N. Hou, Y.-R. Lin, C. W. Liu, *Inorg. Chem.* **2016**, *55*, 3663-3673.

[22] a) C. W. Liu, H.-W. Chang, B. Sarkar, J.-Y.Saillard, S. Kahlal, Y.-Y. Wu, *Inorg. Chem*. **2010**, *49*, 468-475; b) C. W. Liu, H.-W. Chang, C.-S. Fang, B. Sarkar, J.-C. Wang, *Chem. Commun*. **2010**, *46*, 4571-4573; c) C. W. Liu, P.-K. Liaw, C.-S. Feng, J.-Y. Saillard, S. Kahlal, J.-C. Wang, *Chem. Commun*. **2011**, *47*, 5831-5833; d) C. W. Liu, Y.-R. Lin, C.-S. Fang, C. Latouche, S. Kahlal, J.-Y. Saillard, *Inorg. Chem*. **2013**, *52*, 2070-2077; e) C. Latouche, S. Kahlal, Y.-R. Lin, J.-H. Liao, E. Furet, C. W. Liu, J.-Y. Saillard, *Inorg. Chem*. **2013**, *52,*13253-13262; f) C. Latouche, S. Kahlal, E. Furet, P.-K. Liao, Y.-R. Lin, C.-S. Fang, J. Cuny, C. W. Liu, J.-Y. Saillard, *Inorg. Chem*. **2013**, *52*, 7752-7765; g) C. Latouche, C. W. Liu, J.-

Y.Saillard, *J. Clust. Sci*. **2014**, *25*, 147–171; h) J.-H. Liao, H.-W. Chang, Y.-J. Li, C.-S. Fang, B. Sarkar, W. E. van Zyl, C. W. Liu, *Dalton Trans.* **2014**, *43,*12380-12389.

[23] R. S. Dhayal, J.−H. Liao, Y.-C. Liu, M.-H. Chiang, S. Kahlal, J.-Y. Saillard, C. W. Liu, *Angew. Chem. Int. Ed.* **2015**, *54, 3702*-3706; *Angew. Chem.* **2015**, *127*, 3773-3777.

[24] a) M. Walter, J. Akola, O. Lopez-Acevedo, P. D. Jadzinsky, G. Calero, C. J. Ackerson, R. L. Whetten, H. Gronbeck, H. Hakkinen, *Proc. Natl. Acad. Sci. USA* **2008**, *105*, 9157 –9162;b) H. Häkkinen, *Chem. Soc. Rev*. **2008**, *37*, 1847 – 1859; c) B. S. Gutrath, I. B. Oppel, O. Presly, I. Beljakov, V. Meded, W. Wenzel, U. Simon, *Angew. Chem.* **2013**,*125*, 3614 – 3617; *Angew. Chem. Int. Ed.* **2013**, *52*, 3529-3532.

[25] D. Sun, G.-G. Luo, N. Zhang, R.-B. Huang, L.-S. Zheng, *Chem. Commun*. **2011**, *47*, 1461–1463.

[26] A. Bondi, *J. Phys. Chem*. **1964**, *68*, 441–451.

[27] Details of the calculations are provided in the Supporting Information.